FULL PAPER

DOI: 10.1002/ejoc.200((will be filled in by the editorial sttaff))

Synthesis, X-ray Crystal Structures, and Solid-state Fluorescence Properties of Novel 5,5-Dialkyl-9-dibutylamino-5*H*-benzo[*b*]naphtho[1,2-*d*]furan-6-one and 3,3-Dialkyl-9-dibutylamino-3*H*-benzo[*kl*]xanthen-2-one**

Yousuke Ooyama,*[a] Akiko Hayashi,[a] Tomohiro Okamoto,[a] Toshiki Mamura,[a] and Katsuhira Yoshida*[a]

Keywords: Crystal structure / Dyes and pigment / Fluorescence / Heterocycles / Substituent effects

Novel heterocyclic fluorophores, 5,5-dibutyl-9-dibutylamino-5*H*-benzo[*b*]naphtho[1,2-*d*]furan-6-one (**4**) and 3,3-dibutyl-9-dibutylamino-3*H*-benzo[*kl*]xanthen-2-one (**7**) with dialkyl substituent linked non-conjugate to the chromophore skeleton have been derived from the quinol-type compounds **1** and **2** having hydroxyl group, respectively, and their photophysical properties have been investigated in solution and in the solid state. The fluorophores **4** and **7** exhibit strong solid-state fluorescence intensity compared with the quinols **1** and **2**, however, **1** and **4** or **2** and **7** exhibit similar fluorescence intensity in solution. To elucidate the dramatic effect of the dialkyl substituent on the solid-state fluorescence excitation and emission spectra, we have performed the semi-empirical molecular the orbital calculations (AM1 and INDO/S) and X-ray crystallographic analysis. On the basis of the results of the calculations and the X-ray crystal structures, the relations between the solid-state photophysical properties and the chemical and crystal structures of **4** and **7** were discussed. It was confirmed that the introductions of bulky dialkyl disubstituents to the fluorophore skeleton can efficiently prevent the short π-π contact between the fluorophores in molecular aggregation states and cause a dramatic solid-state fluorescence enhancement.

[a] Dr. Y. Ooyama, A. Hayashi, T. Mamura, T. Okamoto, Prof. Dr. K. Yoshida
Department of Material Science, Faculty of Science
Kochi University
Akebono-cho, Kochi 780-8520 (Japan)
Fax: (+81) 88-844-8359
E-mail: kyoshida@cc.kochi-u.ac.jp
yooyama@hiroshima-u.ac.jp

[**] Heterocyclic Quinol-type Fluorophores, Part 8; for Part 7, see: Y. Ooyama, K. Yoshida, *Eur. J. Org. Chem.* **2008**, DOI: 10.1002/ejoc.200800045.

Introduction

In recent years, a great concern has been raised about the enhancement of solid-state fluorescence of organic fluorophores, which is the essential subject for optoelectronics industry such as light emitting diode[1] and photoelectric conversion[2]. Many researches have been conducted on the correlation between the solid-state fluorescence properties and the molecular packing structures on the basis of the X-ray crystal structures. It has been clarified that strong face-to-face intermolecular π-π interaction between parallel neighbouring fluorophores[3–6] or continuous intermolecular hydrogen bonding[4b, 7] was a main factor of fluorescence quenching in the solid state. Consequently, the key point in design of new strong solid-state emissive fluorophores is to remove the intermolecular interactions between fluorophores causing fluorescence quenching in molecular aggregation states. Yamaguchi *et al.* have recently reported that new donor-acceptor-donor type strong solid-state fluorescent dyes, boryl-substituted derivatives having the bulky boryl groups at the side position of fluorophore skeleton inhibit the close packing of the molecules that causes fluorescence quenching.[8] In other cases, Langhals *et al.* and Moorthy *et al.* showed that the introduction of bulky groups to perylene and pyrene skeletons can efficiently inhibit the close packing of their fluorescent molecules, respectively.[9, 10] On the other hand, Ma *et al.* demonstrated that strong supramolecular interaction inducing tight packing and rigid molecules without parallel stacking in crystals of cyano substituent oligo(*para*-phenylene vinylene) are the key factor for the high luminescence efficiency of its crystals.[11] Consequently, It was confirmed that the fluorophores **4** and **7** with bulky 5,5- and 3,3-dibutylsubstituents of non-conjugated linkage to the fluorophore skeleton

In the previous paper, we have reported the synthesis of novel heterocyclic quinols, 5-hydroxy-5-substituent-benzo[*b*]naphtho[1,2-*d*]furan-6-one (**1a**–**1c**) and 3-hydroxy-3-substituent-benzo[*kl*]xanthen-2-one (**2a**–**2c**) fluorophores with substituents (R = Me, Bu and Ph) of non-conjugated linkage to the chromophores and their absorption and fluorescence properties in solution and in the solid state (Scheme 1).[4c] Dramatic substituent effects on the solid-state photophysical properties were observed, which has been elucidated by means of the X-ray crystallographic analysis. It was confirmed that the introduction of 5- and 3-substituents of non-conjugated linkage to the chromophore skeletons of **1** and **2** can efficiently prevent the short π-π contact between the fluorophores in molecular aggregation states and thus cause a dramatic solid-state fluorescence enhancement. On the basis of the results, the introduction of bulky 5,5-disubstituents and 3,3-disubstituents to the chromophore skeletons of **1** and **2**, respectively, would be expected to be more effective for the improvement of the solid-state fluorescence of these fluorophores. In the present paper, we report the photophysical properties in solution and in the crystalline state of new heterocyclic fluorophores,, 5,5-dibutyl-9-dibutylamino-5*H*-benzo[*b*]naphtho[1,2-*d*]furan-6-one (**4**) and 3,3-dibutyl-9-dibutylamino-3*H*-benzo[*kl*]xanthen-2-one (**7**) with bulky 5,5- and

3,3-dibutylsubstituents of non-conjugated linkage to the fluorophore skeleton, respectively. To elucidate the dramatic effect of the dialkyl substituents on the solid-state fluorescence excitation and emission spectra, we have performed the X-ray crystallographic analysis.

Results and Discussion

Synthesis of 5,5-Dibutyl-9-dibutylamino-5*H*-benzo[*b*]naphtho[1,2-*d*]furan-6-one (4) and 3,3-Dibutyl-9-dibutylamino-3*H*-benzo[*kl*]xanthen-2-one (7) Fluorophores

As shown in Scheme 2, we used 5-hydroxy-5-substituent-benzo[*b*]naphtho[1,2-*d*]furan-6-one (**1b**) and 3-hydroxy-3-substituent-benzo[*kl*]xanthen-2-one (**2b**) as starting materials.[4c] The reduction of **1b** and **2b** by using Zn in acetic acid was found to give **3** and **6**, respectively. Next, the heterocyclic fluorophores **4** and **7** were easily obtained by reaction of **3** and **6** with iodobutane by using *t*-butoxylithium, respectively.

Spectroscopic Properties of 1a–1c, 2a–2c, 4, and 7 in Solution

The visible absorption and fluorescence spectral data of **4** and **7** in solution are summarized in Table 1, along with those of **1a**–**1c** and **2a**–**2c**. The fluorescence spectra of the compounds were recorded by excitation at the wavelengths of the longest absorption maximum. The fluorophore **4** exhibits an intense absorption band at around 410 and an intense fluorescence band at around 451 nm in 1,4-dioxane, which are blue-shifted by 10 nm and 25 nm compared with the absorption band and fluorescence band of **1b** in 1,4-dioxane, respectively. The fluorescence quantum yield (Φ) of **4** (Φ = 0.74) is similar to those of the quinols **1a**–**1c**. The absorption spectrum of **4** are little affected by increasing the solvent polarity from 1,4-dioxane to acetonitrile, while these fluorescence spectrum show a large bathochromic shift and a reduction of fluorescence intensity, which were similar to photophysical properties of the quinols **1a**–**1c**. On the other hand, the fluorophore **7** exhibits intense absorption bands at around 407 nm and 427 nm and weak fluorescence band at around 449 nm (Φ = 0.02) in 1,4-dioxane, which are blue-shifted by 10 nm, 7 nm, and 16 nm compared with the absorption band and fluorescence band of **2b** in 1,4-dioxane, respectively. In acetonitrile, the fluorophore **7** exhibits intense absorption bands at around 412 nm and 430 nm and an intense fluorescence band at around 478 nm (Φ = 0.46). The longest absorption maximum of **7** shows a small bathochromic shift of 3 nm from 1,4-dioxane to acetonitrile, while the fluorescence maximum shows a large bathochromic shift of 29 nm. Significant dependence of the fluorescence quantum yield (Φ) on the solvent polarity was also observed: the Φ value of **7** is increased to 23-fold by changing the solvent from 1,4-dioxane to acetonitrile. Similar fluorescence characteristics were previously reported in some aromatic carbonyl compounds such as pyrene-3-carboxaldehyde[12], 7-alkoxycoumarins[13] and *o*-aminoacetophenone[14].

From the above results, owing to the non-conjugated linkage of the substituents (R = Me, Bu and Ph) to the chromophore skeleton, the absorption and fluorescence spectra of the fluorophores **1a**–**1c** and **2a**–**2c** are very similar in each category. However, the hypsochromic shifts were observed in the absorption and fluorescence spectra of the fluorophores **4** and **7**, comparing with those of **1a**–**1c** and **2a**–**2c**, respectively. The hypsochromic shift in the fluorescence spectra is larger than that in the absorption spectra. These results indicate that the differences of the fluorescence spectra between the fluorophores **1a**–**1c** and **4** or **2a**–**2c** and **7** depend on the intramolecular hydrogen-bonding formation. The intramolecular hydrogen-bonding formation is possible for the fluorophores **1a**–**1c** and **2a**–**2c**, but is not for the fluorophores **4** and **7**. A large bathochromic shift of the fluorescence spectra induced by intramolecular hydrogen-bonding formation was previously reported in the fluorophore such as 4-(4-hydroxybenzylidene)-1,2-dimethyl-1*H*-imidazole-5(4*H*)-one.[15] On the other hand, the methoxy derivative, 4-(4-methoxybenzylidene)-1,2-dimethyl-1 *H*-imidazole-5(4*H*)-one which can not form the intramolecular hydrogen-bonding, emits in hypsochromic region compared to the above hydroxyl compound.

Semi-empirical MO calculations (AM1, INDO/S) of 1a–1c, 2a–2c, 4, and 7 in Solution

The photophysical spectra of the compounds **1a**–**1c**, **2a**–**2c**, **4**, and **7** were analyzed by using semi-empirical molecular orbital (MO) calculations. The molecular structures were optimized by using MOPAC/AM1 method[16], and then the INDO/S method[17] was used for spectroscopic calculations. The calculated absorption wavelengths and the transition character of the first absorption bands are collected in Table 2. The calculated absorption wavelengths and the oscillator strength values are relatively good compatible with the observed spectra in 1,4-dioxane, although the calculated absorption spectra are blue shifted. The deviation of the INDO/S calculations, giving transition energies greater than the experimental values, has been generally observed.[18] The calculations explain well that the calculated absorption spectra of the quinols **1a**–**1c** or **2a**–**2c** resemble each other very well, because of the non-conjugated linkage of the substituents (R = Me, Bu, and Ph) to the chromophore skeleton. The calculated absorption wavelengths of **4** and **7** are blue shifted compared with those of **1a**–**1c** and **2a**–**2c**, respectively, which is good compatible with the observed spectra in solution. Furthermore, the calculated oscillator strengths (*f*) of the compounds **1a**–**1c** and **4** or **2a**–**2c** and **7** are almost identical in each category, which is also good compatible with the observed spectra in solution.

For the compounds **1a**–**1c** and **4**, the calculations show that the longest excitation bands for the four compounds are mainly assigned to the transition from the HOMO to the LUMO, where HOMO were mostly localized on the *p*-dibutylaminobenzofurano moiety, and the LUMO were mostly localized on the naphthoquinol moiety. On the other hand, for the compounds **2a**–**2c** and **7**, the calculations also show that the longest excitation bands for the four compounds are mainly assigned to the transition from the HOMO to the LUMO, where HOMO are mostly localized on the *p*-dibutylaminobenzopyran moiety, and the LUMO were mostly localized on the naphthoquinol moiety. The calculated electron density changes accompanying the first electron excitation are shown in Figure 2, which shows a strong migration of intramolecular charge-transfer character of **1a**–**1c**, **2a**–**2c**, **4**, and **7**.

The values of the dipole moments in the grand states are 7.35 for **1a**, 6.17 for **1b**, 6.98 for **1c**, 6.52 for **4**, 7.21 for **2a**, 7.03 for **2b**, 7.10 for **2c**, and 6.34 for **7**. The differences between the dipole moments ($\Delta\mu$) of the first excited and the ground states are 7.52 for **1a**, 5.91 for **1b**, 7.23 for **1c**, and 6.10 for **4**, 6.47 for **2a**, 6.32 for **2b**, 5.93 for **2c**, and 6.24 for **7**. These calculations indicate that the compounds **1a**–**1c** and **4** or **2a**–**2c** and **7** have similar large dipole moments in the excited state, which explains well the experimental observations that the these compounds show a large bathochromic shift of their fluorescence maxima in polar solvents and that the Stokes shift values for the these compounds in acetonitrile are much larger than those in 1,4-dioxane.

Spectroscopic Properties of 1a–1c, 4, 2a–2c, and 7 in the Solid State

Interesting results have been obtained by comparing the photophysical properties of the crystals **4** and **7** with those of the crystals **1a**–**1c** and **2a**–**2c**. Figure 1 shows that the optical properties of **1a**–**1c** and **4** or **2a**–**2c** and **7** are quite different between the solution and the solid state. The crystal of **4** exhibits strong blue fluorescence emission, but the crystals of **1a**, **1b**, and **1c** exhibit relatively weak yellowish-orange, green, and greenish-yellow fluorescence emission, respectively. On the other hand, the crystal of **7** exhibits strong greenish-yellow emission, while the crystals of **2a**, **2b**, and **2c** exhibit relatively weak yellowish-orange, green, and red emissions, respectively. In order to investigate the difference in the solid-state photophysical properties among **1a**–**1c** and **4** or **2a**–**2c** and **7**, we have measured the fluorescence excitation and emission spectra of the crystals. Figures 3 and 4 show the spectroscopic properties of **1a**–**1c** and **4** or **2a**–**2c** and **7** in the crystalline state. The fluorescence intensity of **1a**–**1c** and **4** are in the order of **4** > **1c** > **1b** > **1a** in the crystalline state: the fluorescence intensity of **4** is ca. 5-fold larger than that of **1b**. The wavelengths of the emission maximum of **1a** (λ_{em} = 560 nm), **1b** (λ_{em} = 530 nm), **1c** (λ_{em} = 555 nm), and **4** (λ_{em} = 480 nm) are red-shifted by 84, 54, 70, and 29 nm compared with that in 1,4-dioxane, respectively. It is noteworthy that the emission maximum of **4** in the solid state is similar to that in 1,4-dioxane.

On the other hand, the fluorescence intensity of **2a**–**2c** and **7** are in the order of **7** > **2b** > **2a** > **2c** in the crystalline state. The longest wavelengths of the excitation and the emission maxima of **7** (λ_{ex} = 470 nm, λ_{em} = 500 nm) in the crystalline state are red-shifted by 43 and 51 nm compared with those of **7** in 1,4-dioxane, respectively. In contrast, the longest wavelengths of the excitation and the emission maxima of **2b** (λ_{ex} = 497 nm, λ_{em} = 529 nm) in the crystalline state are large red-shifted by 63 and 64 nm compared with those of **2b** in 1,4-dioxane, respectively. These results demonstrated that the solid-state photophysical properties of **4** and **7** having dialkyl substituent are approaching their photophysical properties in solution.

X-ray Crystal Structures of 1a–1c, 4, 2a–2c, and 7

In the previous paper, we have demonstrated that the substituents (R = Me, Bu, Ph) of the quinols **1a**–**1c** and **2a**–**2c** greatly affect the geometric arrangement in the crystal structure.[4c] In **1a**, **1b** and **2c**, the interplanar distance between the fluorophores is short because the substituent (methyl group in **1a**, butyl group in **1b**, and phenyl group in **2c**) and the 9-dibutylamino group are located on the same side of the π plane, and the molecules are packed in the structural form with table shape (Figure 9). The large red-shift of the absorption and fluorescence maxima and the solid-state fluorescence quenching in the crystals of **1a** and **2c** are considered to be induced by strong donor-acceptor type π-π interactions.[3f, 4 5] On the other hand, in **1c**, **2a** and **2b**, the molecules are packed in the structural form with a stepped-shape because the substituent (phenyl group in **1c**, methyl group in **2a**, and butyl group in **2b**) and the 9-dibutylamino group are located on opposite sides of the molecular π plane (Figures 5 and 6). Therefore, the interplanar distance between the fluorophores is longer (Figure 9) so that the π-π interactions are weakened by the substituents thus leading stronger solid-state fluorescence emission.

From these results, the introductions of bulky 5,5-disubstituents and 3,3-disubstituents to the chromophore skeletons of **1** and **2**, respectively, should prevent more efficiently the short π-π contact between the fluorophores in molecular aggregation states. To elucidate the dramatic substituent effect on the solid state photophysical properties, the X-ray crystal structures of the **4** and **7** have been determined and shown in Figures 7 and 8. The crystal systems of these compounds are summarized in Tables 3. The packing structures demonstrate that the molecules are arranged in a "herring-bone" fashion both in the crystals of **4** and **7**. In the case of the two dialkyl derivatives, there are no intermolecular hydrogen bonds between the enantiomers. As we expected, the crystal structure of **4** has only one edge-to-edge interatomic contacts (O(1)···C(77) 3.207(4) Å) of less than 3.60 Å between the neighboring fluorophores in the crystal structure (Figure 7). In the crystal of **7**, on the other hand, a π-stacking of the fluorophores was formed in one cluster unit in which π-overlappings were observed partially between the chromene moiety and the 9-dibutylaminobenzo moiety of the adjacent fluorophores. The inclination between the benzoxanthenone planes in the pair of equal enantiomers is 17° (Figure 8(c)). Furthermore, continuous π stacking of the equal enantiomers formed in the crystal structures of **2a** and **2b** and strong donor-acceptor π stacking formed in the crystal structures of **2c** were not observed in the crystal structure of **7**. As evident by comparing the crystal structure of **7** with those of **2a**–**2c**, the range of π-stacking of **7** is much less than that of those of **2a**–**2c**. These results demonstrate that the introduction of dialkyl substituents to fluorophores effectively prevents the intermolecular π–π interaction and intermolecular hydrogen bonding between fluorophores causing a large red-shift of the absorption and fluorescence maxima and fluorescence quenching in the solid state.

In the crystals of **4** and **7**, the molecules are packed in the structural form with a chair-shape. Therefore, the interplanar distance between the fluorophores is longer (Figure 9), so that the π-π interactions are weakened by the disubstituents, leading stronger solid-state fluorescence emission. From these results, we propose a favorable stereostructure for the solid-state fluorescence. For example, the H-shaped fluorophores with four bulky substituents which are located on both sides of the π plane, leading to inhibition of the π-π interactions between the fluorophores, would exhibit not only the strong solid-state fluorescence but also exhibit almost the same fluorescence properties in solution and in the solid state.

Conclusions

We have synthesized heterocyclic fluorophores, 5,5-Dibutyl-9-dibutylamino-5*H*-benzo[*b*]naphtho[1,2-*d*]furan-6-one (**4**) and 3,3-Dibutyl-9-dibutylamino-3*H*-benzo[*kl*]xanthen-2-one (**7**) having bulky dialkyl substituents linked non-conjugate to the chromophore skeleton have been derived from the quinol-type compounds **1** and **2** and their photophysical properties have been investigated in solution and in the solid state. Dramatic dialkyl substituent effects on the solid-state photophysical properties were observed, which has been elucidated by means of the X-ray crystallographic analysis. It was confirmed that the fluorophores **4** and **7** with bulky 5,5- and 3,3-dibutylsubstituents of non-conjugated linkage to the fluorophore skeleton can efficiently prevent the short π-π contact between the fluorophores causing fluorescence quenching in the solid state.

Experimental Section

General: Melting points were measured with a Yanaco micro melting point apparatus MP-500D. IR spectra were recorded on a JASCO FT/IR-5300 spectrophotometer for samples in KBr pellet form. Absorption spectra were observed with a JASCO U-best30 spectrophotometer and fluorescence spectra were measured with a JASCO FP-777 spectrophotometer. Single-crystal X-ray diffraction was performed on Rigaku AFC7S diffractometer. For the measurement of the solid-state fluorescence excitation and emission spectra of the crystals, a JASCO FP-777 spectrometer equipped with a JASCO FP-1060 attachment was used. The fluorescence quantum yields

(Φ) for **1a**–**1c** and **2a**–**2c** were determined by using 9,10-bis(phenylethynyl)anthracene (Φ = 0.84, λ_{ex} = 440 nm)[19] in benzene as the standard. The fluorescence quantum yields (Φ) for **4** and **7** were determined by using 9,10-diphenylanthracene (Φ = 0.67, λ_{ex} = 357 nm)[19] in benzene as the standard. Elemental analyses were recorded on a Perkin Elmer 2400 II CHN analyzer. ^{1}H NMR spectra were recorded on a JNM-LA-400 (400 MHz) FT NMR spectrometer with tetramethylsilane (TMS) as an internal standard. Column chromatography was performed on silica gel (KANTO CHEMICAL, 60N, spherical, neutral).

Synthesis of 5,5-dibutyl-9-dibutylamino-5*H*-benzo[*b*]naphtho[1,2-*d*]furan-6-one (4): A mixed solution (70 ml) of **1b** (0.70 g, 1.61 mmol) and Zn powder (1.29 g, 24.2 mmol) in acetic acid was refluxed for 6 h. The reaction mixture was filtrate and the filtrate was evaporated and the residue was extracted with CH_2Cl_2. The organic extract was washed with water and then evaporation of the solvent afforded a mixture of **3** as white solid, which is unstable to air. A mixture of **3** and iodbutane (2.97 g, 16.1 mmol) and *tert*-butoxylithium (1.42 g, 17.8 mmol) was stirred at 130 °C for 20 h. The reaction mixture was extracted with CH_2Cl_2. The organic extract was washed with water and neutralized by NH_4Cl aqueous solution. The organic extract was evaporated and the residue was chromatographed on silica gel (CH_2Cl_2 : as eluent) to give **4** (0.44g, yield 57%) as a yellow powder; crude compound **3**: ^{1}HNMR(400 MHz, [D_6]acetone, TMS) δ = 0.94-1.72 (21H, m), 3.25 (2H, t), 3.48 (4H, t), 6.84-6.86 (2H, m), 6.74-6.76 (2H, m), 8.02-8.16 (2H, m), 8.44-8.47 (1H, m); compound **4**: mp 149-150 °C; ^{1}HNMR(400 MHz, [D_3]chloroform, TMS) δ = 0.60-1.16 (24H, m), 1.34-1.43 (4H, m), 1.57-1.67(4H, m), 1.82-2.38 (4H, m), 3.47 (4H, t , J = 7.32 Hz), 6.76 (1H, d, J = 2.2 Hz), 6.82 (1H, dd, J = 9.0 and 2.2 Hz), 7.40-7.50 (4 H, m), 8.01 (1H, d, J = 9.0 Hz) 8.10 (1H, dd, J = 6.6 and 2.44 Hz); IR (KBr) $\tilde{\nu}$ = 1617 cm^{-1}; elemental analysis calcd (%) for $C_{32}H_{43}NO_2$ (473.69): C 81.14, H 9.15, N 2.96; found: C 81.33, H 9.16, N 2.92.

Synthesis of 3,3-Dibutyl-9-dibutylamino-3*H*-benzo[*kl*]xanthen-2-one (7): A mixed solution (150 ml) of **2b** (1.59 g, 3.67 mmol) and Zn powder (3.62 g, 55.0 mmol) in acetic acid was refluxed for 2 h. The reaction mixture was filtrate and the filtrate was evaporated and the residue was extracted with CH_2Cl_2. The organic extract was washed with water and then evaporation of the solvent afforded a mixture of **6** as white solid, which is unstable to air. A mixture of **6** and iodbutane (6.75 g, 36.7 mmol) and *tert*-butoxylithium (4.40 g, 55.0 mmol) was stirred at 130 °C for 20 h. The reaction mixture was extracted with CH_2Cl_2. The organic extract was washed with water and neutralized by NH_4Cl aqueous solution. The organic extract was evaporated and the residue was chromatographed on silica gel (CH_2Cl_2 : as eluent) to give **7** (0.44g, yield 25%) as a yellow powder; crude compound **6**: ^{1}HNMR(400 MHz, [D_3]chloroform, TMS) δ = 0.95-1.68 (21H, m), 2.86 (2H, t), 3.36 (4H, t), 6.40-6.61 (2H, m), 6.67-6.77 (1H, m), 6.98-7.06 (1H, m), 7.27-7.43 (3H, m); compound **7**: mp 111-112 °C; ^{1}H NMR (400 MHz, [D_6]acetone, TMS) δ = 0.68-1.17 (16H, m), 1.38-1.70 (m, 12H), 1.82-2.12 (m, 4H), 3.50 (4H, t), 6.33 (s, 1H), 6.47 (d, J = 2.44 Hz, 1H), 6.79 (dd, J = 2.44 and 9.04 Hz, 1H), 7.16 (d, J = 8.0 Hz, 1H), 7.36 (d, J = 8.0 Hz, 1H), 7.57 (t, J = 8.0 Hz,1H),7.84 (d, J = 9.04 Hz, 2H); IR (KBr) $\tilde{\nu}$ = 1597 cm^{-1}; elemental analysis calcd (%) for $C_{32}H_{43}NO_2$ (473.69): C 81.14, H 9.15, N 2.96; found: C 81.42, H 9.39, N 2.93.

X-ray crystallographic studies: The reflection data were collected at 23 ± 1°C on a Rigaku AFC7S four-circle diffractometer by 2θ-ω scan technique, and using graphite-monochromated $Mo_{K\alpha}$ (λ = 0.71069 Å) radiation at 50 kV and 30 mA. In all case, the data were corrected for Lorentz and polarization effects. A correction for secondary extinction was applied. The reflection intensities were monitored by three standard reflections for every 150 reflections. An empirical absorption correction based on azimuthal scans of several reflections was applied. All calculations were performed using the teXsan[20] crystallographic software package of Molecular Structure Corporation. CCDC-294660 (**1a**), CCDC-294661 (**1b**), CCDC-294662 (**1c**) CCDC-294192 (**2a**), CCDC-294193 (**2b**), CCDC-294194 (**2c**), CCDC-652309 (**4**), and CCDC-652310 (**7**) contain the supplementary crystallographic data for this paper. These data can be obtained free of charge via www.ccdc.cam.au.uk/data_request/cif.

Compound 4: Crystals of **4** were recrystallized from *n*-hexane and given as yellow prism, air stable. The one selected had approximate dimensions 0.80×0.66×0.43 mm. The transmission factors ranged from 0.93 to 1.00. The crystal structure was solved by direct methods using SIR 92.[21] The structures were expanded using Fourier techniques.[22] The non-hydrogen atoms were refined anisotropically. Some hydrogen atoms were refined isotropically, the rest were fixed geometrically and not refined. **Crystal data:** $C_{32}H_{43}NO_2$, M = 473.70, triclinic, a = 11.689(2), b = 17.905(7), c = 28.309(5) Å, α = 79.75(2)°, β = 93.56(2)°, γ = 95.65(2)°, U = 5795(2) Å^3, T = 296.2K, space group $P\bar{1}$ (no.2), Z = 8, $\mu(Mo_{K\alpha})$ = 0.66 cm^{-1}, 27900 reflections measured, 26601 unique (R_{int} = 0.024) which were used in all calculations. The final R indices [$I > 2\sigma(I)$], $R1$ = 0.063, $wR(F^2)$ = 0.144.

Compound 7: Crystals of **7** were recrystallized from *n*-hexane and given as yellow prism, air stable. The one selected had approximate dimensions 0.55×0.35×0.50 mm. The transmission factors ranged from 0.93 to 1.00. The crystal structure was solved by direct methods using SIR 92.[21] The structures were expanded using Fourier techniques.[22] The non-hydrogen atoms were refined anisotropically. Some hydrogen atoms were refined isotropically, the rest were fixed geometrically and not refined. **Crystal data:** $C_{32}H_{43}NO_2$, M = 473.70, monoclinic, a = 37.767(8), b = 11.080(2), c = 14.074(4) Å, β = 98.74(2)°, U = 5820(3) Å^3, T = 296.2K, space group $P2_1/n$ (no.14), Z = 8, $\mu(Mo_{K\alpha})$ = 0.66 cm^{-1}, 10990 reflections measured, 10238 unique (R_{int} = 0.059) which were used in all calculations. The final R indices [$I > 2\sigma(I)$], $R1$ = 0.060, $wR(F^2)$ = 0.179.

Computational methods: All calculations were performed on FUJITSU FMV-ME4/657. The semi-empirical calculations were carried out with the WinMOPAC Ver. 3 package (Fujitsu, Chiba, Japan). Geometry calculations in the ground state were carried out using the AM1 method.[16] All geometries were completely optimized (keyword PRECISE) by the eigenvactor following routine (keyword EF). Experimental absorption spectra of the compounds were studied with the semi-empirical method INDO/S (intermediate neglect of differential overlap/spectroscopic).[17] All INDO/S calculations were performed using single excitation full SCF/CI (self-consistent field/configuration interaction), which includes the configuration with one electron excited from any occupied orbital to any unoccupied orbital, 225 configurations were considered for the configuration interaction [keyword CI (15 15)].

Acknowledgments

This work was partially supported by a Grant-in-Aid for Science and Research from the Ministry of Education, Science, Sport and Culture of Japan (Grant 18350100), by a Science and Technology Incubation Program in Advanced Regions of Japan Science and Technology Agency (JST), and by a Special Research Grant for Green Science from Kochi University.

[1] a) C. W. Tang, S. A. VansSlyke, *Appl. Phys. Lett*. **1987**, *51*, 913–915; b) C. W. Tang, S. A. VansSlyke, C. H. Chen, *J. Appl. Phys*. **1989**, *65*, 3610–3616; c) J. Schi, C. W. Tang, *Appl. Phys. Lett*. **1997**, *70*, 1665–1667; d) A. Kraft, A. C. Grimsdale, A. B. Holmes, *Angew. Chem*. **1998**, *110*, 416–443; *Angew. Chem. Int. Ed*. **1998**, *37*, 402–428; e) U. Mitschke, P. Bäuerle, *J. Mater. Chem*. **2000**, *10*, 1471–1507; f) K.-C. Wong, Y. -Y. Chien, R.-T. Chen, C.-F. Wang, Y.-T. Liu, H.-H. Chiang, P.-Y. Hsieh, C.-C. Wu, C. H. Chou, Y. O. Su, G.-H. Lee , S.-M. Peng, *J. Am. Chem. Soc*. **2002**, *124*, 11576–11577; g) C. J. Tonzola, M. M. Alam, W. K. Kaminsky, S. A. Jenekhe, *J. Am. Chem. Soc*. **2003**, *125*, 13548–13558; h) H.-C. Yeh, L.-H. Chan, W.-C. Wu, C.-T. Chen, *J. Mater. Chem*. **2004**, *14*, 1293–1298; i) C.-T. Chen, *Chem. Mater*. **2004**, *16*, 4389–4400; j) C.-L. Chiang, M.-F. Wu, D.-C. Dai, Y.-S. Wen, J.-K. Wang, C.-T. Chen, *Adv. Funct.*

Mater. **2005**, *15*, 231–238; k) D. Berner, C. Klein, M. D. Nazeeruddin, F. de Angelis, M. Castellani, P. Bugnon, R. Scopelliti, L. Zuppiroli, M. Graetzel, *J. Mater. Chem*. **2006**, *16*, 4468–4474.

[2] a) Z.-S. Wang, F.-Y. Li, C.-H. Hang, L. Wang, M. Wei, L.-P. Jin, N.-Q. Li, *J. Phys. Chem. B* **2000**, *104*, 9676–9682; b) A. Ehret, L. Stuhl, M. T. Spitler, *J. Phys. Chem. B* **2001**, *105*, 9960–9965; c) K. Hara, T. Sato, R. Katoh, A. Furube, Y. Ohga, A. Shinpo, S. Suga, K. Sayama, H. Sugihara, H. Arakawa, *J. Phys. Chem. B* **2003**, *107*, 597–606; d) K. R. J. Thomas, J. T. Kin, Y.-C. Hsu, K.-C. Ho, *Chem. Commun*. **2005**, 4098–4100; e) D. P. Hagberg, T. Edvinsson, T. Marinado, G. Boschloo, A. Hagfeld, L. Sun, *Chem. Commun*. **2006**, 2245–2247; f) S.-L. Li, K.-J. Jiang, K.-F. Shao, L.-M. Yang, *Chem. Commun*. **2006**, 2792–2794.

[3] a) K. Hirano, S. Minakata, M. Komatsu, *Chem. Lett*. **2001**, 8–9; b) Y. Sonoda, Y. Kawanishi, T. Ikeda, M. Goto, S. Hayashi, N. Tanigaki, K. Yase, *J. Phys. Chem. B* **2003**, *107*, 3376–3383; c) R. Davis, S. Abraham, N. P. Rath, S. Das, *New J. Chem*. **2004**, *28*, 1368–1372; d) V. de Halleux, J.-P. Calbert, P. Brocorens, J. Cornil, J.-P. Declercq, J.-L. Brédas, Y. Geerts, *Adv. Funct. Mater*. **2004**, *14*, 649–659; e) H.-C. Yeh, W.-C. Wu, Y.-S. Wen, D.-C. Dai, J.-K. Wang, C.-T. Chen, *J. Org. Chem*. **2004**, *69*, 6455–6462; f) E. Horiguchi, S. Matsumoto, K. Funabiki, M. Matsui, *Bull. Chem. Soc. Jpn*. **2005**, *78*, 1167–1173; g) S. Mizukami, H. Houjou, K. Sugaya, E. Koyama, H. Tokuhisa, T. Sasaki, M. Kanesato, *Chem. Mater*. **2005**, *17*, 50–56; h) Y. Mizobe, N. Tohnai, M. Miyata, Y. Hasegawa, *Chem. Commun.* **2005**, 1839–1841; i) I. Vayá, M. C. Jiménez, M. Miranda, *Tetrahedron: Asymmetry* **2005**, *16*, 2167–2171; j) Z. Xie, B. Yang, L. Liu, M. li, D. Lin, Y. Ma, G. Cheng, S. Liu, *J. Phys. Org. Chem*. **2005**, *18*, 962–973; k) Y. Ooyama, Y. Harima, *Chem. Lett*., **2006**, 902–903; l) Y. Ooyama, Y. Kagawa, Y. Harima, *Eur. J. Org. Chem*., **2007**, 3613–3621.

[4] a) K. Yoshida, Y. Ooyama, M. Miyazaki, S. Watanabe, *J. Chem. Soc. Perkin Trans. 2*, **2002**, 700–707; b) Y. Ooyama, T. Nakamura, K. Yoshida, *New J. Chem*. **2005**, *29*, 447–456; c) Y. Ooyama, T. Okamoto, T. Yamaguchi, T. Suzuki, A. Hayashi, K. Yoshida, *Chem.-Eur. J.* **2006**, 7827–7838; d) Y. Ooyama, T. Mamura, K. Yoshida, *Tetrahedron Letters* **2007**, 5791–5793: e) Y. Ooyama, T. Mamura, K. Yoshida, *Eur. J. Org. Chem.* **2007**, *30*, 5010–5019.

[5] a) K. Yoshida, J. Yamazaki, Y. Tagashira, S. Watanabe, *Chem. Lett*. **1996**, 9–10; b) K. Yoshida, T. Tachikawa, J. Yamasaki, S. Watanabe, S. Tokita, *Chem. Lett*. **1996**, 1027–1028; c) K. Yoshida, H. Miyazaki, Y. Miura, Y. Ooyama, S. Watanabe, *Chem. Lett*. **1999**, 837–838; d) K. Yoshida, Y, Ooyama, S. Tanikawa, S. Watanabe, *Chem. Lett*. **2000**, 714–715; e) K. Yoshida, Y. Ooyama, S. Tanikawa, S. Watanabe, *J. Chem. Soc. Perkin Trans. 2* **2002**, 708–714; (f) Y. Ooyama, K. Yoshida, *New J. Chem*. **2005**, *29*, 12041212.

[6] H. Langhals, T. Potrawa, H. Nöth, G. Linti, *Angew. Chem*. **1989**, *101*, 497–499; *Angew. Chem. Int. Ed. Engl*. **1989**, *28*, 478–480.

[7] K. Yoshida, K. Uwada, H. Kumaoka, L. Bu, S. Watanabe, *Chem. Lett*. **2001**, 808–809.

[8] C.-H. Zhao, A. Wakamiya, Y. Inukai, S. Yamaguchi, *J. Am. Chem. Soc*. **2006**, *128*, 15934–15935.

[9] H. Langhals, R. Ismael, O. Yürük, *Tetrahedron* **2001**, *56*, 5435–5441.

[10] J. N. Moorthy, P. Natarajan, P. Venkatakrishnan, D.-F. Huang, T. J. Chow, *Org. Lett*. **2007**, *9*, 5215–5218.

[11] Y. Li, F. Li, H. Zhang, Z. Xie, W. Xie, H. Xu, B. Li, F. Shen, L. Ye, M. Hanif, D. Ma, Y. Ma, *Chem. Commun*. **2007**, 231–233.

[12] K. Kalyanasundaram and J. K. Thomas, *J. Phys. Chem*. **1977**, *81*, 2176–2180.

[13] B. Valeur, *Molecular Fluorescence*, VCH, Weinheim, **2002**.

[14] T. Yoshihara, H. Shimada, H. Shizuka and S. Tobita, *Phys. Chem. Chem. Phys*. **2001**, *3*, 4972–4978.

[15] K.-Y. Chen, Y.-M. Cheng, C.-H. Lai, C.-C. Hsu, M.-L. Ho, G.-H. Lee, P.-T. Chou, *J. Am. Chem. Soc*. **2007**, *129*, 4534–4535.

[16] M. J. S. Dewar, E. G. Zoebisch, E. F. Healy, J. J. P. Stewart, *J. Am. Chem. Soc.* **1985**, ***107***, 3902–3909.

[17] a) J. E. Ridley, M. C. Zerner, *Theor. Chim. Acta* **1973**, *32*, 111–134; b) J. E. Ridley , M. C. Zerner, *Theor. Chim. Acta* **1976**, *42*, 223–236; c) A. D. Bacon, M. C. Zerner, *Theor. Chim. Acta* **1979**, *53*, 21–54.

[18] a) M. Adachi, Y. Murata, S. Nakamura, *J. Org. Chem.* **1993**, *58*, 5238–5244; b) W. M. F. Fabian, S. Schuppler, O. S. Wolfbeis, *J. Chem. Soc., Perkin Trans. 2* **1996**, 853–856.

[19] C. A. Heller, R. A. Henry, B. A. Mclaughlin, D. E. Bills, *J. Chem. Eng. Data* **1974**, *19*, 214–219.

[20] teXsan: Crystal Structure Analysis Package, Molecular Structure Corporation **1985** and **1992**.

[21] A. Altomare, M. C. Burla, M. Camalli, M. Cascarano, C. Giacovazzo, A. Guagliardi, G. Polidori, *J. Appl. Cryst*. **1994**, *27*, 435–.

[22] DIRDIF94. P. T. Beurskens, G. Admiraal, G. Beurskens, W. P. Bosman, R. de Gelder, R. Israel, J. M. M. Smits, The DIRIF94 program system, Technical Report of the Crystallography Laboratory, University of Nijmegen, The Netherlands, **1994**.

Received: ((will be filled in by the editorial staff))
Published online: ((will be filled in by the editorial staff))

Entry for the Table of Contents (Please choose one layout)

Layout 1:

Dramatic dialkyl substituent effects on the solid-state photophysical properties of novel heterocyclic fluorophores, 5,5-Dibutyl-9-dibutylamino-5*H*-benzo[*b*]naphtho[1,2-*d*]furan-6-one (**4**) and 3,3-Dibutyl-9-dibutylamino-3*H*-benzo[*kl*]xanthen-2-one (**7**), have been discussed on the basis of the X-ray crystal structures.

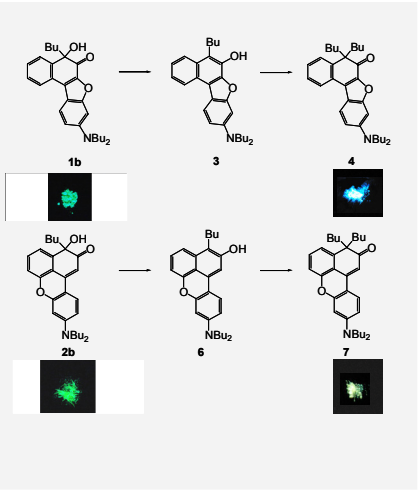

Y. Ooyama*, A. Hayashi, T. Okamoto, T. Mamura, K. Yoshida*

…….. Page No. – Page No.

Synthesis, X-ray Crystal Structures, and Solid-state Fluorescence Properties of Novel 5,5-Dialkyl-9-dibutylamino-5*H*-benzo[*b*]naphtho[1,2-*d*]furan-6-one and 3,3-Dialkyl-9-dibutylamino-3*H*-benzo[*kl*]xanthen-2-one

Keywords: Crystal structure / Dyes and pigment / Fluorescence / Heterocycles / Substituent effects

Table 1. Absorption and fluorescence spectral data of **1a**–**1c**, **2a**–**2c**, **4**, and **7** in solution

		Absorption	Fluorescence		SS[a]
	Solvent	λ_{max} [nm] (ε_{max} [$dm^3mol^{-1}cm^{-1}$])	λ_{max} [nm]	Φ	$\Delta\lambda_{max}$ [nm]
1a	Benzene	427 (22500)	470	0.76	43
	1,4-Dioxane	421 (21300)	476	0.74	55
	THF	419 (20900)	494	0.60	75
	DMF	426 (20200)	524	0.35	98
	DMSO	430 (20400)	528	0.31	98
	Acetonitrile	428 (20500)	524	0.30	96
	Ethanol	432 (20400)	538	0.16	106
1b	1,4-Dioxane	420 (21700)	476	0.74	56
	Acetonitrile	430 (22600)	525	0.31	95
1c	1,4-Dioxane	430 (21600)	484	0.74	55
	Acetonitrile	441 (22400)	536	0.30	95
4	1,4-Dioxane	410 (25200)	451	0.73	41
	THF	409 (24700)	464	0.56	55
	Acetonitrile	415 (24100)	497	0.27	82
2a	Cyclohexane	430(30200), 408(32500)	441	0.03	11
	Diethyl ether	430(28400), 411(31300)	457	0.04	27
	1,4-Dioxane	433(29400), 416(28200)	464	0.04	31
	THF	433(29700), 419(31100)	479	0.14	46
	DMF	438(29200)	503	0.27	65
	DMSO	441(28700)	506	0.27	65
	Acetonitrile	438(32600)	501	0.46	63
	Ethanol	442(33200)	508	0.33	66
2b	1,4-Dioxane	434(29000), 417(28000)	465	0.04	31
	Acetonitrile	440(32400)	501	0.43	61
2c	1,4-Dioxane	442(31200), 426(30700)	472	0.03	30
	Acetonitrile	450(35300)	507	0.43	57
7	1,4-Dioxane	427(32100), 407(34600)	449	0.02	22
	THF	427(30300), 408(32300)	455	0.08	28
	Acetonitrile	430(32200), 412(32400)	478	0.46	48

[a] Stokes shift value.

Table 2. Calculated absorption spectra for the compounds **1a**–**1c**, **2a**–**2c**, **4**, and **7**

Quinol	Absorption (calc.)				
	μ [D][a]	λ_{max} [nm]	f[b]	CI component [c]	$\Delta\mu$ [D][d]
1a	7.35	362	0.48	HOMO→LUMO (89%)	7.52
1b	6.17	367	0.42	HOMO→LUMO (89%)	5.91
1c	6.98	355	0.46	HOMO→LUMO (89%)	7.23
4	6.52	353	0.48	HOMO→LUMO (88%)	6.10
2a	7.21	342	0.74	HOMO→LUMO (86%)	6.47
2b	7.03	343	0.74	HOMO→LUMO (86%)	6.32
2c	7.10	346	0.71	HOMO→LUMO (86%)	5.93
7	6.34	335	0.74	HOMO→LUMO (86%)	6.24

[a] The values of the dipole moment in the ground state. [b] Oscillator strength. [c] The transition is shown by an arrow from one orbital to another, followed by its percentage CI (configuration interaction) component. [d] The values of the difference in the dipole moment between the excited and the ground states.

Table 3. Crystal data and structure refinement parameter for the compounds **4** and **7**

Compound	**4**	**7**
Molecular formula	$C_{32}H_{43}NO_2$	$C_{32}H_{43}NO_2$
Formula weight	473.70	473.70
Number of reflection for unit cell Cell determination(2θ range/°)	23 (25.0-33.0)	16 (22.2-24.2)
Crystal System	triclinic	monoclinic
Space group	$P\bar{1}$	$P2_1/n$
a/Å	11.689(2)	37.767(8)
b/Å	17.905(7)	11.080(4)
c/Å	28.309(5)	14.074(4)
α/°	79.75(2)	
β/°	93.56(2)	98.74(2)
γ/°	95.65(3)	
V/ Å^3	5795(2)	5820(3)
Z	8	8
Dc/g cm^{-3}	1.086	1.081
F(000)	2064.00	2064.00
M(Mokα)/cm^{-1}	0.66	0.66
Crystal dimensions/nm	0.80x0.66x0.43	0.55x0.35x0.50
Scan mode	*ω*-2*θ*	*ω*-2*θ*
Scan rate in ω/°min^{-1}	8.0-16.0 (up to 5 scans)	8.0-16.0 (up to 7 scans)
Scan wide/°	1.47 + 0.30tan*θ*	1.21 + 0.30tan*θ*
2*θ* max/°	55.0	50.0
Range of induces *h*; *k*; *l*	0, 15; -23, 23; -36, 36	0, 44; -13, 0; -16, 16
Reflection collected (unique)	26601	10238
Reflection observed with $I_0>2\sigma I_0$	6697	3491
Number of parameters	1262	632
R	0.063	0.060
Rw	0.144	0.179
W	$(\sigma^2F^2)^{-1}$	$(\sigma^2F^2)^{-1}$
S	1.26	1.25
Max. Shift/Error in final cycle	0.029	0.015
Max. Peak in final diff. map/e Å^{-3}	0.54	0.27
Min. Peak in final diff. map/e Å^{-3}	-0.55	-0.23

Figure and Scheme captions

Scheme 1. Heterocyclic quinol-type fluorophores **1a**–**1c** and **2a**–**2c**.

Scheme 2. Synthesis of **4** and **7**. a) Zn, CH_3COOH, reflux, 2-6 h; b) *t*BuOLi, *n*BuI, 130°C, 20h, 57% for **4**, 25% for **7**.

Figure 1. Fluorescence properties of **1a**–**1c**, **2a**–**2c**, **4**, and **7** (a) in solution (1,4-dioxane for **1a**–**1c** and **4**; DMSO for **2a**–**2c** and **7**) and (b) in the solid state.

Figure 2. Calculated electron density changes accompanying the first electronic excitation of **1b**, **2b**, **4**, and **7**. The black and white lobes signify the decrease and increase in electron density accompanying the electronic transition. Their areas indicate the magnitude of the electron density change.

Figure 3. Solid-state excitation (···) and emission (—) spectra of the crystals of **1a**–**1c** and **4**; **1a**: λ_{ex} = 510 nm, λ_{em} = 560 nm; **1b**: λ_{ex} = 503 nm, λ_{em} = 530 nm; **1c**: λ_{ex} = 519 nm, λ_{em} = 555 nm; **4**: λ_{ex} = 454 nm, λ_{em} = 480 nm.

Figure 4. Solid-state excitation (···) and emission (—) spectra of the crystals of **2a**–**2c** and **7**; **2a**: λ_{ex} = 514 nm, λ_{em} = 564 nm; **2b**: λ_{ex} = 497 nm, λ_{em} = 529 nm; **2c**: λ_{ex} = 550 nm, λ_{em} = 608 nm; **7**: λ_{ex} = 470 nm, λ_{em} = 500 nm.

Figure 5. Crystal packing pattern of **1a**–**1c** (a) a side view, and (b) a top view of the pairs of fluorophores.

Figure 6. Crystal packing pattern of **2a**–**2c** (a) a side view, and (b) a top view of the pairs of fluorophores.

Figure 7. Crystal packing of **4** (a) a stereoview of the molecular packing structure, (b) a schematic structure, (c) a side view, and (d) a top view of the pairs of fluorophores.

Figure 8. Crystal packing of **7** (a) a stereoview of the molecular packing structure, (b) a schematic structure, (c) a side view, and (d) a top view of the pairs of fluorophores.

Figure 9. Schematic representation of the effects of the substituents on interplanar distances between a pair of fluorophores for **1a**–**1c**, **2a**–**2c**, **4** and **7**.

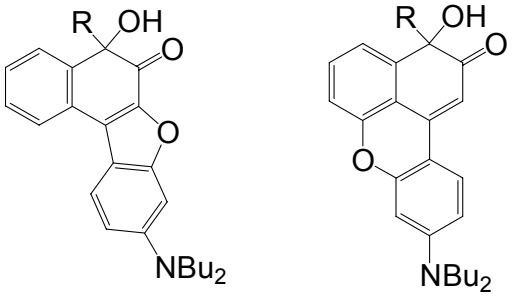

1a: R=Me
1b: R=Bu
1c: R=Ph

2a: R=Me
2b: R=Bu
2c: R=Ph

Scheme 1

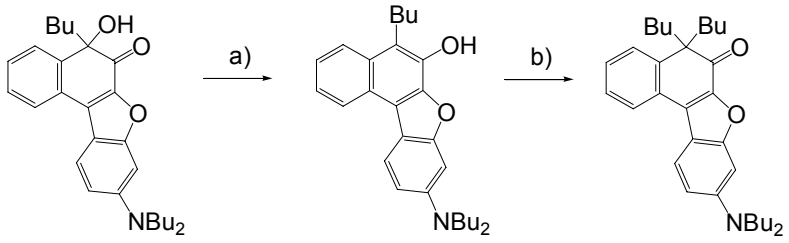

1b **3** **4**

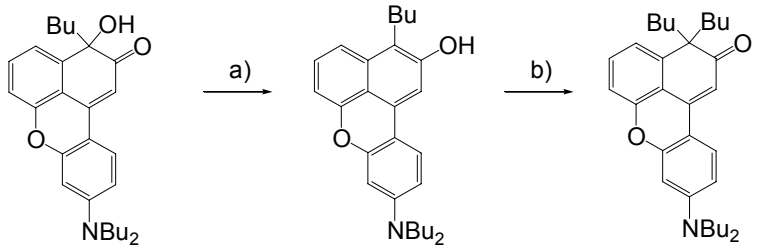

2b **6** **7**

Scheme 2

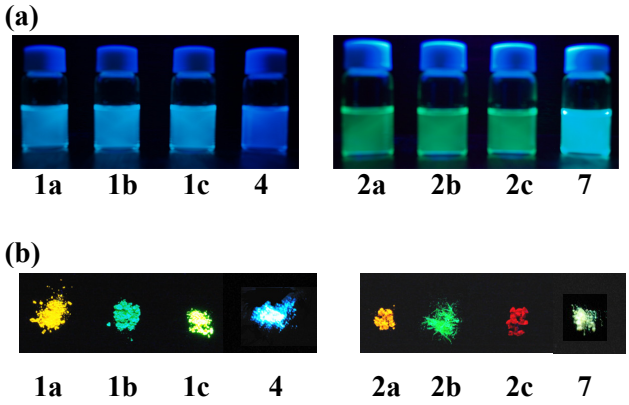

Figure 1

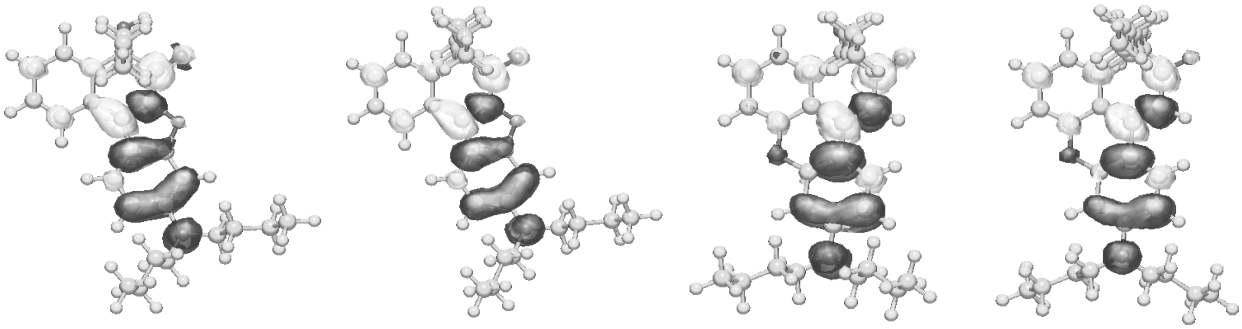

Figure 2

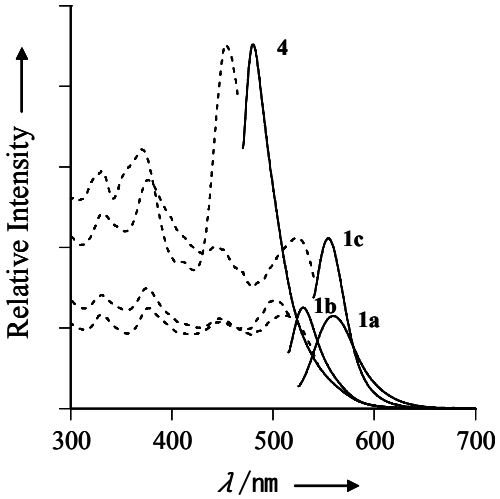

Figure 3

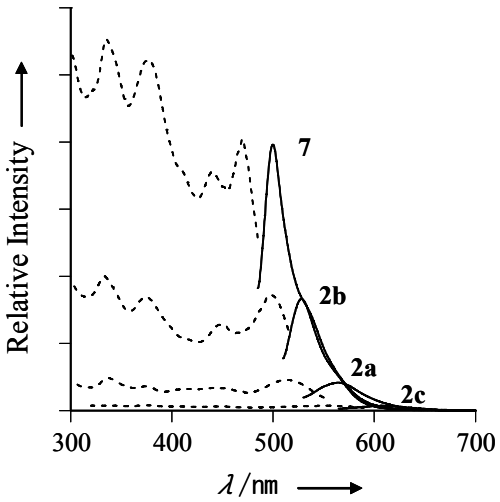

Figure 4

(a)

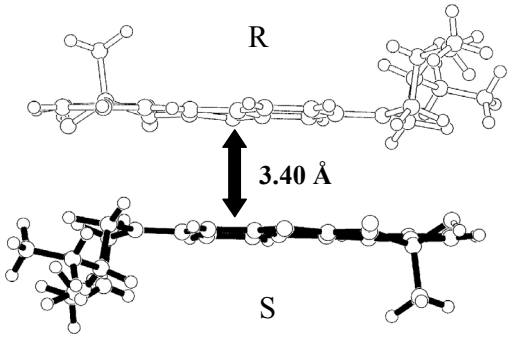

1a

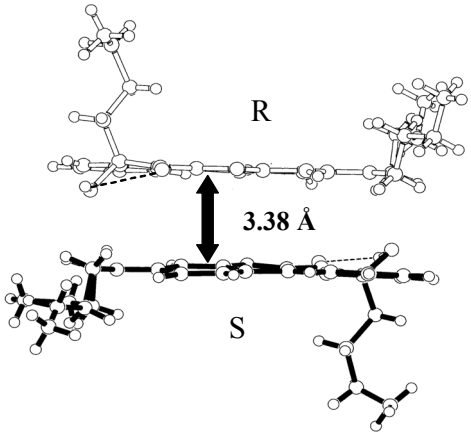

1b

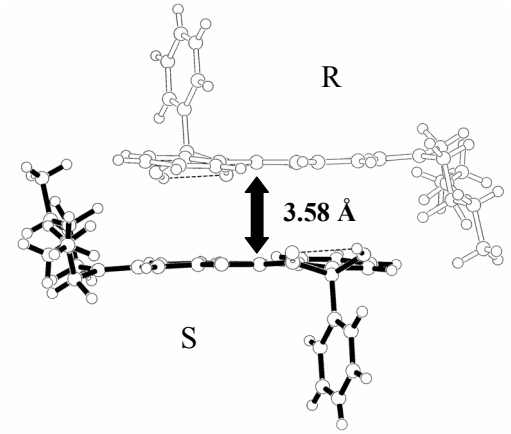

1c

(b)

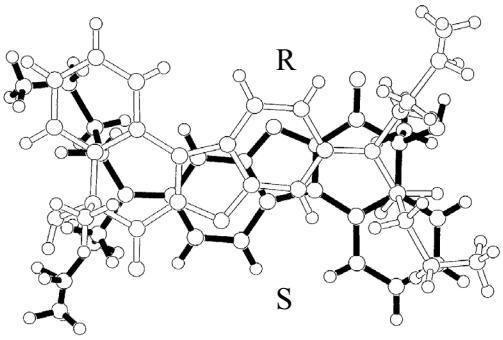

1a

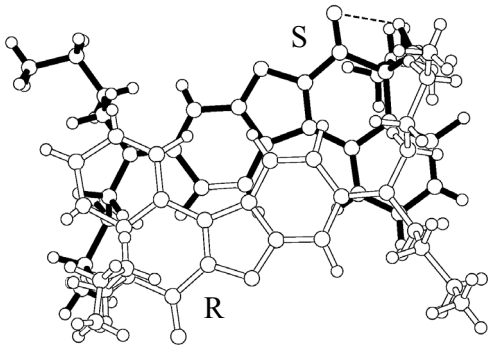

1b

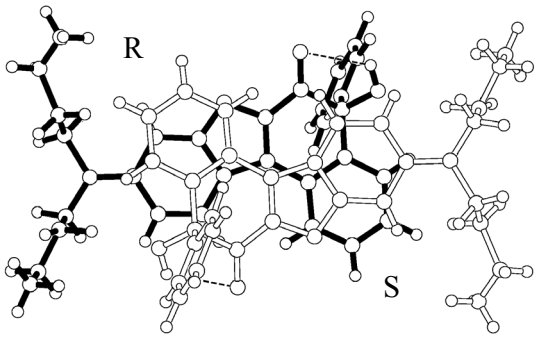

1c

Figure 5

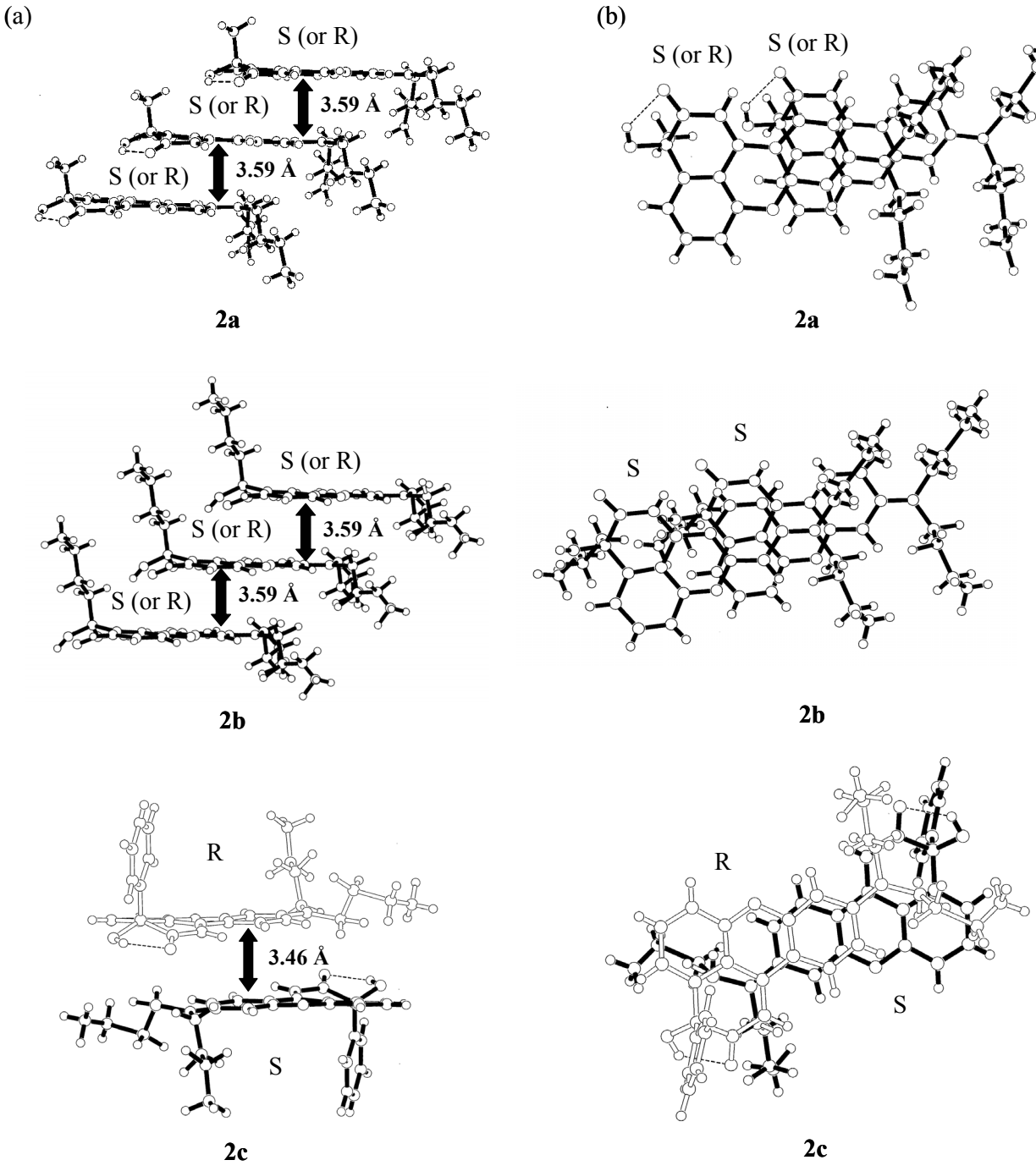
(a)
S (or R)
S (or R)
3.59 Å
S (or R)
3.59 Å
2a
(b)
S (or R)
S (or R)
2a
S (or R)
S (or R)
3.59 Å
S (or R)
3.59 Å
2b
S
S
2b
R
3.46 Å
S
2c
R
S
2c

Figure 6

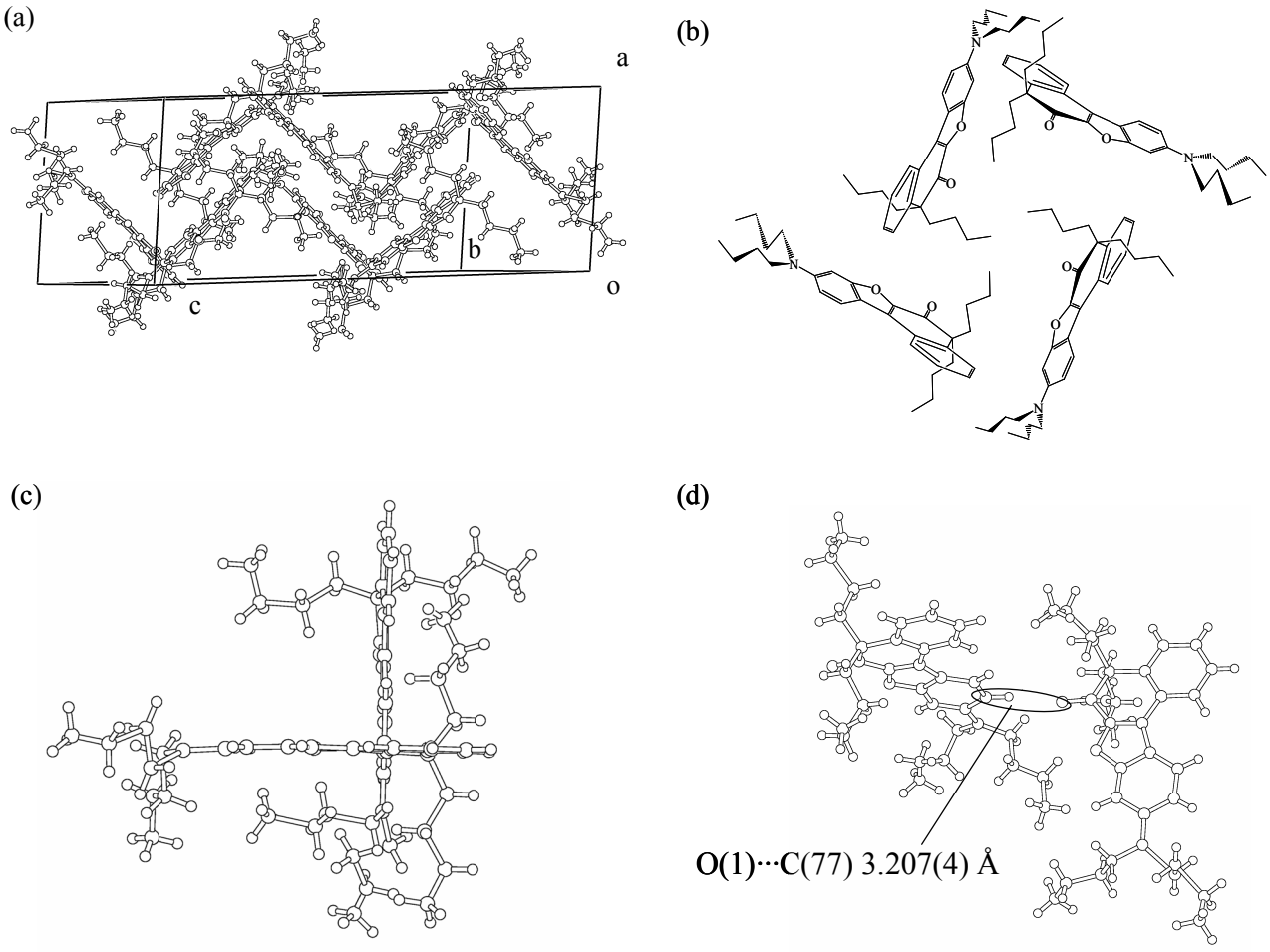

Figure 7

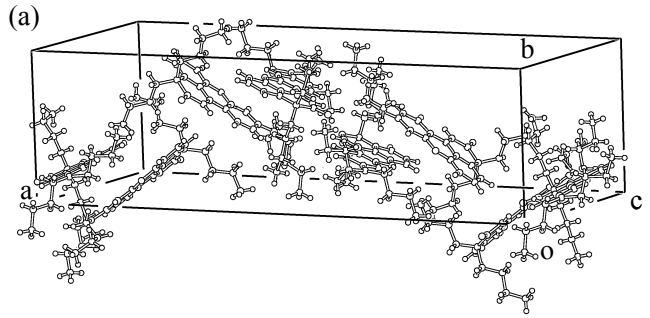

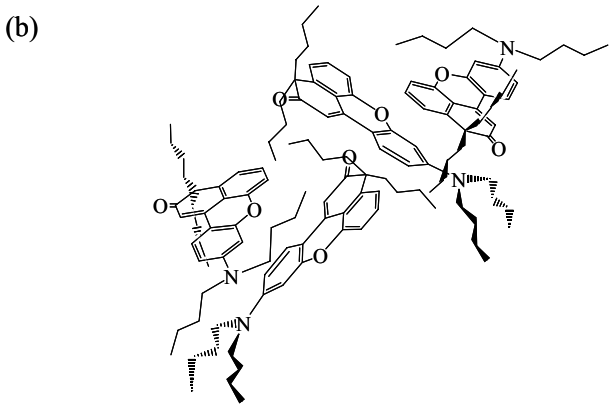

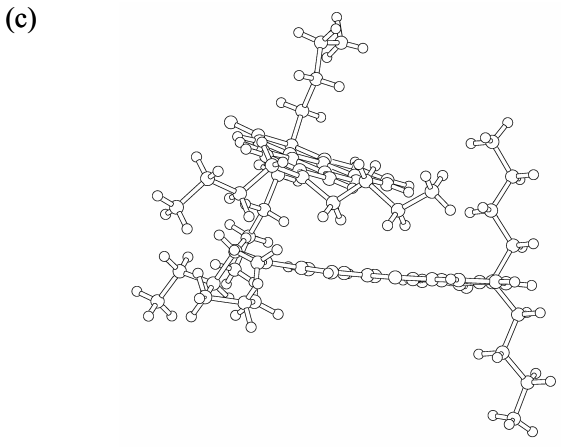

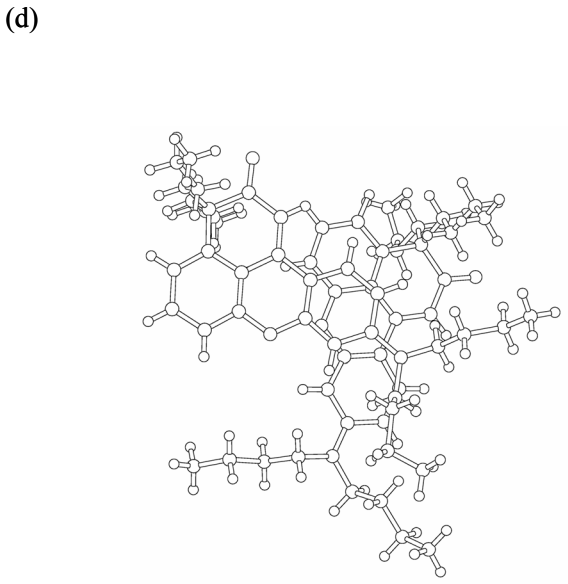

Figure 8

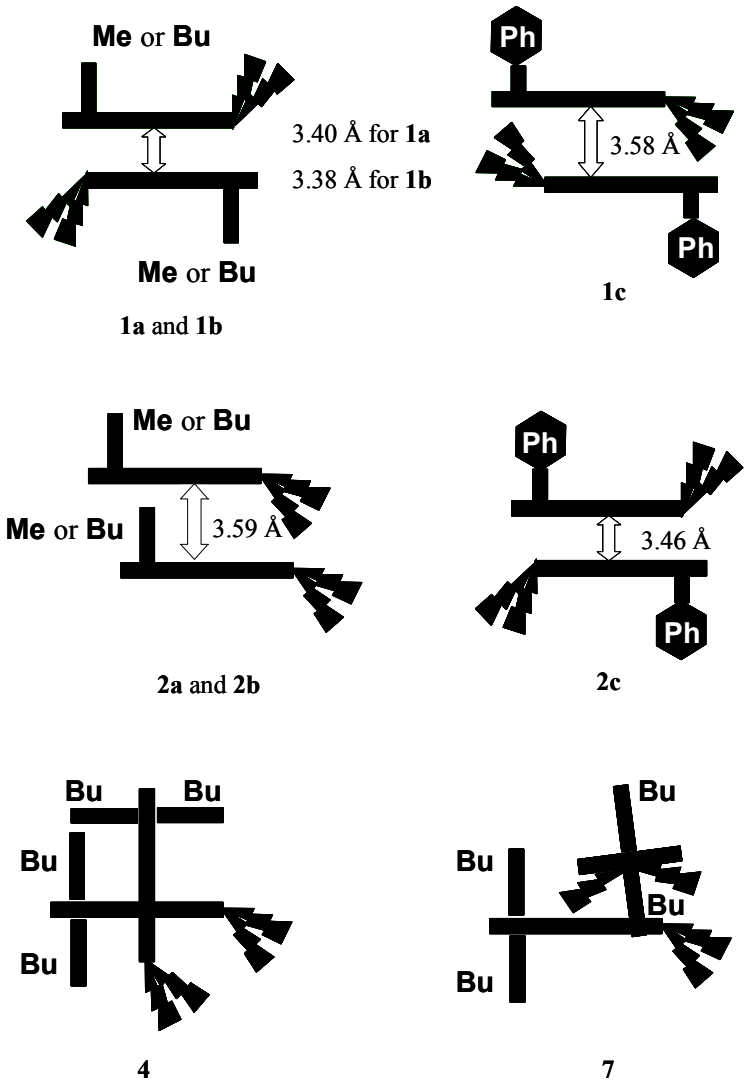
Me or Bu
3.40 Å for 1a
3.38 Å for 1b
Me or Bu
1a and 1b
Ph
3.58 Å
Ph
1c
Me or Bu
Me or Bu
3.59 Å
2a and 2b
Ph
3.46 Å
Ph
2c
Bu
Bu
Bu
Bu
4
Bu
Bu
Bu
Bu
7

Figure 9